PROJECT 1 REPORT: TRANSIENT THERMAL ANALYSIS OF A DYNAMIC COOLING LOOP

1.0. Introduction

High-power electronic systems such as AI data centers, electric vehicles, and industrial power systems increasingly depend on active liquid cooling, as these liquids (often water–glycol) have higher effective thermal conductivity and heat capacity than air, enabling reliable cooling at power densities that would overwhelm air-cooled designs (Thermtest, 2024; Williams, 2012). Liquid-cooling loops use cold plates, rear-door or rack-level heat exchangers, and pumps to transport heat away from critical components, supporting server rack densities on the order of 80–200+ kW per rack, far beyond typical air-cooled limits of roughly 10–15 kW per rack in conventional facilities (Gramont, 2026; Kadhim, 2018).

This project presents a lumped-capacity MATLAB/Simulink model of a dynamic cooling loop, with a core goal of capturing how coolant flow rate, heat exchanger performance, and heat input interact over time. Two critical scenarios are investigated, alongside the base model, to understand how transient overshoots and steady-state temperatures respond to disturbances to the system to provide insights for real-world deployments in data centers, electric vehicles, and industrial systems:

- **Scenario A** (Pump Failure): A sudden reduction in mass flow rate (0.2kg/s to 0.01kg/s at 1000s).
- **Scenario B** (Efficiency Improvement): Doubling the radiator's overall conductance, UA_{rated} (150W/K to 300W/K).

2.0. Simulink Model

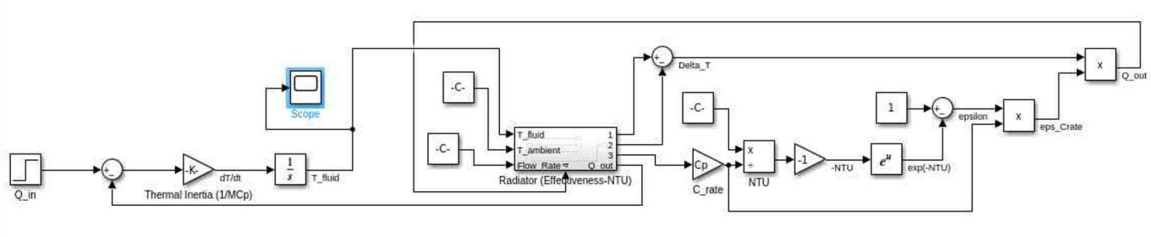

Figure 1: Base Model of the Dynamic Cooling Loop (Simulink)

2.1. Model Description

The Simulink model (CoolingLoopModel.slx) comprises four main subsystems:

- **Heat Input Block** (Step Input): Heat load steps from 0 to 1000W at t=10s.
- **Radiator Subsystem** (Effectiveness-NTU): This computes Q_{out} using the ε–NTU equation ($Q_{\text{out}} = \epsilon\, C_{\text{rate}}(T_{\text{fluid}} - T_{\text{ambient}})$. Details of the computation are shown in the Model Calculation and Theories subsection.
- **Lumped-Capacity Integrator**: This integrates the net heat, $Q_{\text{in}} - Q_{\text{out}}$ divided by thermal mass MC_p to obtain T_{fluid}, using a Sum block and a Gain block feeding an Integrator.
- **Scopes and Data Logging**: Scopes display $T_{\text{fluid}}(t)$ and, in Scenario A, the flow-rate trajectory $\dot{m}(t)$. Signal logging is enabled so that the full responses can be exported and plotted.

2.2. Parameters

The base model simulation utilizes the following parameters, as shown in the MATLAB script (setup_cooling_loop.m):

Parameters	Values	Unit
Coolant density (ρ)	1000	kg/m^3
Coolant volume (V)	0.02	m^3
Total fluid mass (M)	20	kg
Specific heat capacity (C_p)	3500	J/(kg·K)
Thermal mass (MC_p)	70,000	J/K
Nominal flow rate ($\dot{m}$)	0.2	kg/s
Radiator UA (Base, Scenario A)	150	W/K
Radiator UA (Scenario B)	300	W/K
Ambient temperature (T_{ambient})	25	°C
Initial coolant temperature (T_{init})	25	°C
Heat load (Q)	1000	W
Heat load step time (t)	10	s

Table 1: Model parameters for all simulation runs

Above are representative engineering values leveraging typical liquid-cooling hardware and standard property data. The parameters were selected to keep loop temperatures in the 30–55°C range typical for electronics and battery cooling to match realistic operating bands for data centers, electric vehicles, and industrial thermal management systems (Gramont, 2026; Kadhim, 2018; Neural Concept, 2026; Thermtest, 2024). Coolant properties were chosen to represent a typical water–glycol mixture (ρ ≈ 1000 kg/m^3, $C_p \approx 3.5$ kJ/kg·K), consistent with standard property tables for 30–50% ethylene glycol solutions near 20–30°C (CoreChem, 2026; The Engineering ToolBox, 2003; EAI Water, 2026; Melinder, 2007). Nominal mass flow rate was set to 0.2 kg/s (≈12 L/min), which lies within the range of flow rates reported for liquid-cooled electronics plates and manifolds (1–10 L/min, depending on power and channel design) (SinoExtrud, 2025; Chandra & Ramakrishna, 2013; Williams, 2012). The Scenario A value of 0.01 kg/s was made extreme to simulate a severe failure and stress the system. Radiator conductance was set to 150 W/K (base) and 300 W/K (improved), values representative of compact liquid-to-air heat exchangers handling kW-scale loads with temperature lifts of 5–10°C (PA Hilton, 2026; Williams, 2012). Moreover, the coolant volume, fluid mass, and heat load were chosen as realistic values for the potential industrial applications

2.3. Model Calculation and Theories

The cooling loop is modeled as a single, well-mixed thermal mass exchanging heat with a finite-capacity heat source and an external heat sink (radiator). The formulation below follows the lumped-capacitance and heat-exchanger methods presented in Lienhard and Lienhard's A Heat Transfer Textbook (6th Ed.), and explains how each part of the Simulink diagram implements those calculations from the heat input Q_{in} to the heat rejected Q_{out} and the resulting coolant temperature T_{fluid}.

A. Lumped Thermal Mass and Energy Balance: Here, the standard first-order lumped capacity model for transient conduction and well-mixed systems is applied.

For a control volume containing coolant of mass m and specific heat C_p, with uniform temperature $T_{\text{fluid}}(t)$, the unsteady energy balance can be written in lumped form as:

$$mC_p \frac{dT_{\text{fluid}}}{dt} = Q_{\text{in}}(t) - Q_{\text{out}}(t)$$

Here:

- $Q_{\text{in}}(t)$is the heat rate from the electronics
- $Q_{\text{out}}(t)$is the heat rate rejected to the ambient air via the radiator

In the Simulink diagram, the $\boldsymbol{Q}_{\text{in}}$ Step block applies a 1 kW step at $t = 10$s. A **Sum** block subtracts the computed $Q_{\text{out}}$to form the net heat rate $Q_{\text{net}} = Q_{\text{in}} - Q_{\text{out}}$. The block labeled **Thermal inertia (1/MCp)** multiplies this by $1/(mC_p)$, directly implementing:

$$\frac{dT_{\text{fluid}}}{dt} = \frac{Q_{\text{in}} - Q_{\text{out}}}{mC_p}$$

The **Integrator** block then integrates $\frac{dT_{\text{fluid}}}{dt}$ in time with initial condition $T_{\text{fluid}}(0) = T_{\text{ambient}}$, yielding the state variable $T_{\text{fluid}}(t)$.

B. Radiator Heat-Exchanger Model (ε–NTU method): The radiator subsystem uses the **effectiveness–NTU** formulation introduced in the heat-exchangers chapter of *A Heat Transfer Textbook*.

For a single-phase heat exchanger with coolant heat-capacity rate $C_{\text{rate}} = \dot{m}C_p$, overall conductance UA, and capacity ratio $C_r = C_{\min}/C_{\max}$, Lienhard & Lienhard define the number of transfer units as:

$$\text{NTU} = \frac{UA}{C_{\min}}$$

and the effectiveness ϵ as the ratio of actual to maximum possible heat transfer:

$$\epsilon = \frac{Q_{\text{out}}}{Q_{\max}}$$

For the configuration modeled here, the ambient air side is treated as having a very large heat-capacity rate relative to the coolant, so $C_{\min} = C_{\text{rate}}$ and $C_r \to 0$. In this special case, the ε–NTU relations simplify to:

$$\epsilon = 1 - e^{-\text{NTU}}, \text{NTU} = \frac{UA_{\text{rated}}}{\dot{m}C_p}$$

and the maximum possible heat transfer becomes $Q_{\max} = C_{\min}(T_{\text{fluid}} - T_{\text{ambient}})$. The actual radiator heat-rejection rate is therefore:

$$Q_{\text{out}} = \epsilon\, \dot{m}C_p\, (T_{\text{fluid}} - T_{\text{ambient}})$$

The Simulink radiator subsystem implements these steps explicitly:

i. **Temperature difference**
The top feedback line carries T_{fluid} into the radiator. A **Sum** block subtracts the constant ambient temperature to form:

$$\Delta T = T_{\text{fluid}} - T_{\text{ambient}}$$

ii. **Capacity rate**
The flow-rate input $\dot{m}$ is multiplied by C_p in the **Cp** Gain block, giving:

$$C_{\text{rate}} = \dot{m}C_p$$

iii. **NTU**

The **NTU** block divides the parameter UA_{rated} by C_{rate}:

$$\text{NTU} = \frac{UA_{\text{rated}}}{C_{\text{rate}}}$$

iv. **Effectiveness**

A Gain block forms −NTU, which feeds an **exp(-NTU)** block to compute $e^{-\text{NTU}}$. A subsequent **Sum** block subtracts this from 1, producing:

$$\epsilon = 1 - e^{-\text{NTU}}$$

v. **Effective conductance and Q_{out}**

The block labeled **eps_Crate** multiplies ϵ and C_{rate}, yielding $\epsilon \dot{m} C_p$. The final product block multiplies this by ΔT, generating:

$$Q_{\text{out}} = \epsilon \dot{m} C_p (T_{\text{fluid}} - T_{\text{ambient}})$$

This Q_{out} signal is fed back to the main energy-balance sum, so the radiator performance directly influences the subsequent evolution of T_{fluid}.

C. Resulting First-Order Dynamics: Substituting the ε–NTU expression for Q_{out}into the lumped energy balance shows that, for constant $Q_{\text{in}}$and $\dot{m}$, the loop behaves as a **first-order linear system**:

$$mC_p \frac{dT_{\text{fluid}}}{dt} = Q_{\text{in}} - \epsilon(\dot{m})\dot{m}C_p(T_{\text{fluid}} - T_{\text{ambient}})$$

For a step in heat load, Lienhard & Lienhard show that such systems respond as:

$$T_{\text{fluid}}(t) = T_\infty + (T_0 - T_\infty)\, e^{-t/\tau}$$

with steady state and time constant:

$$T_\infty = T_{\text{ambient}} + \frac{Q_{\text{in}}}{\epsilon \dot{m} C_p}, \tau = \frac{m}{\epsilon \dot{m}}$$

The Simulink model does not solve these formulas analytically; instead, it integrates the differential equation numerically. However, the block-level calculations from Q_{in}through the ε–NTU radiator to $Q_{\text{out}}$and T_{fluid}correspond directly to the methodology and equations presented in the Lienhard & Lienhard Heat Transfer Textbook, 6th edition.

2.4. Simulation Scenarios

As mentioned earlier, alongside the base model, two distinct scenarios are considered, with the model simulated for 3600s, and $T_{\text{fluid}}(t)$ recorded:

A. Base Model
   - $\dot{m} = 0.2$ kg/s
   - $UA_{\text{rated}} = 150$ W/K

B. Scenario A (Pump Failure)
   - Replace the Constant block driving $\dot{m}$ with a Step block.
   - Step time, $t_s = 1000$ s.
   - Initial value, 0.2 kg/s

- Final value, 0.01 kg/s

C. Scenario B (Efficiency Improvement)
- $\dot{m} = 0.2$ kg/s
- In setup_cooling_loop.m, change UA_{rated} from 150W/K to 300W/K.
- Rerun the script so the updated parameter is utilized by Simulink.

3.0. Results

Below are the results for the base model, Scenario A and Scenario B.

3.1. Base Model Results

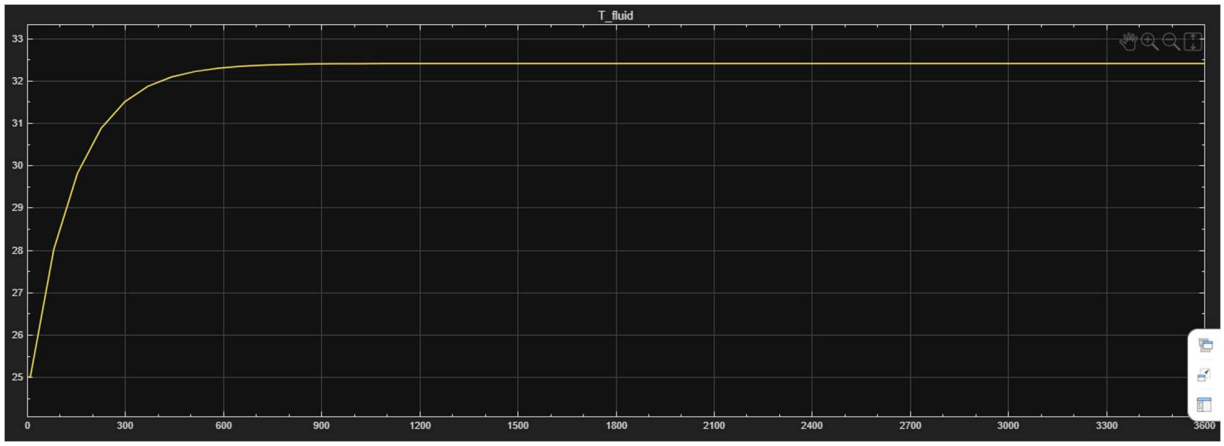

Figure 2: T_{fluid} vs t of the Base Model

After the heat step to 1 kW at 10 s, the coolant temperature rises from 25°C and asymptotically approaches a steady value around 32.4°C. The curve is monotonic and exhibits classic first-order behavior. This is consistent with the analytical steady-state prediction:

- $C_{\text{rate}} = \dot{m}C_p = 0.2 \times 3500 = 700$ W/K
- NTU $= \frac{150}{700} \approx 0.214$
- $\epsilon = 1 - e^{-0.214} \approx 0.193$
- $\epsilon C_{\text{rate}} \approx 0.193 \times 700 \approx 135$ W/K
- Steady-state from $Q_{\text{in}} = Q_{\text{out}}$:

$$1000 = \epsilon C_{\text{rate}}(T_\infty - 25) \Rightarrow T_\infty - 25 \approx \frac{1000}{135} \approx 7.41^\circ\text{C}$$
$$T_\infty \approx 32.4^\circ\text{C}$$

The Scope plot matches this calculation to within plotting resolution, validating that the ε–NTU and lumped-capacity implementations are correct.

3.2. Scenario A (Pump Failure) Results

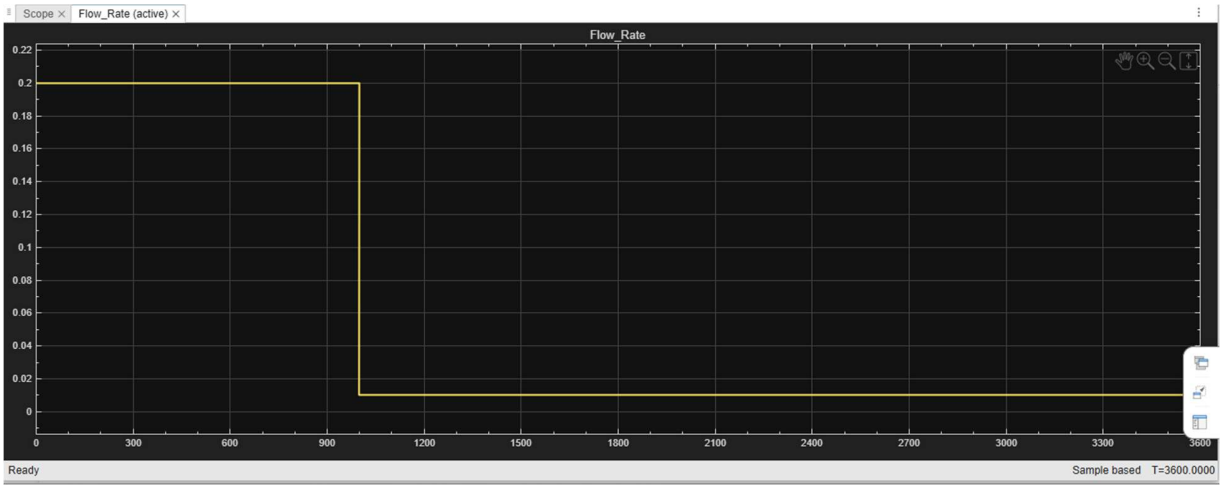

Figure 3: Flow Rate in Scenario A Model

Figure 3 above shows the flow rate trajectory:

- $\dot{m} = 0.2$ kg/sfor $0 < t < 1000$ s.
- At $t = 1000$ s, a step down to $\dot{m} = 0.01$ kg/s.

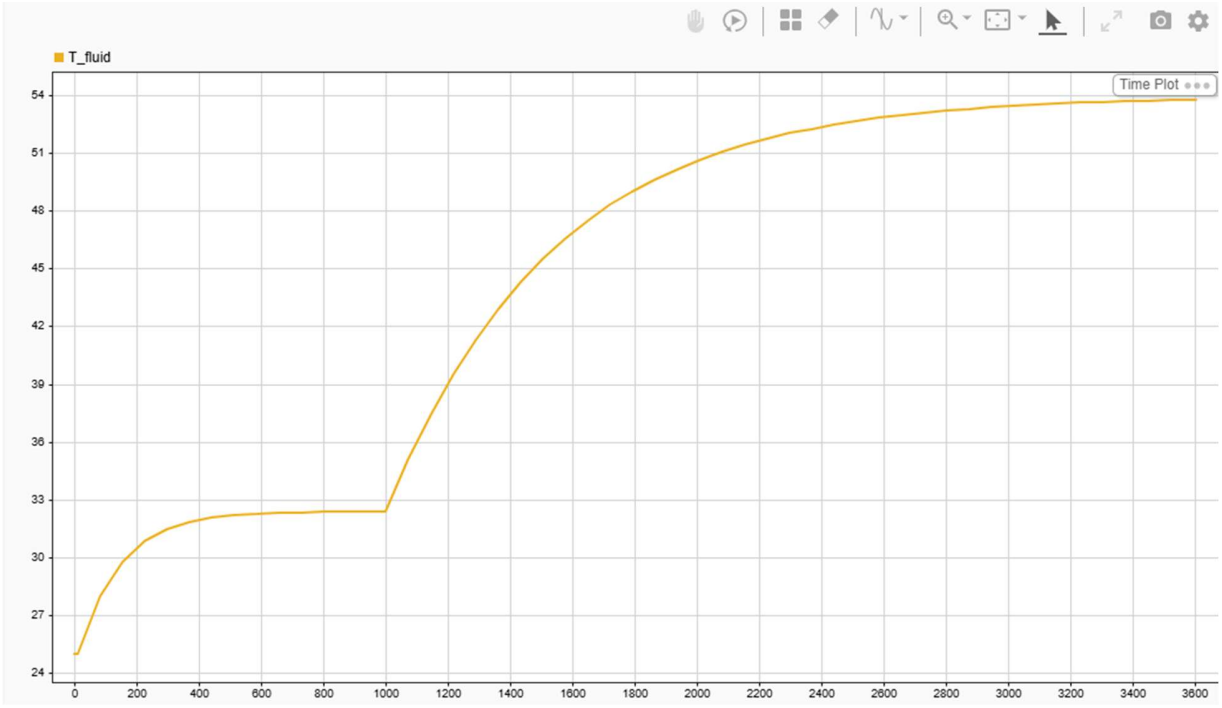

Figure 4: T_{fluid} vs t of the Scenario A Model

Figure 4 shows the corresponding coolant temperature response:

A. From 10 s to about 1000 s, the system behaves identically to the base case, rising from 25°C toward ~32.4°C.

B. At 1000 s, when the pump "fails" and flow collapses to 0.01 kg/s, the radiator loses most of its cooling capacity. The model exhibits:
    a. A distinct kink in the temperature trace.
    b. A renewed, much steeper rise in T_{fluid}.
C. Over the following ~30–40 minutes, T_{fluid} climbs toward a new steady-state value around 54°C.

The new steady-state can again be calculated analytically:

- New $C_{\text{rate}} = 0.01 \times 3500 = 35$ W/K
- NTU $= 150/35 \approx 4.29$
- $\epsilon = 1 - e^{-4.29} \approx 0.986$
- $\epsilon C_{\text{rate}} \approx 0.986 \times 35 \approx 34.5$ W/K
- Steady-state:

$$1000 = 34.5(T_\infty - 25) \Rightarrow T_\infty - 25 \approx 29°\text{C} \Rightarrow T_\infty \approx 54°\text{C}$$

The simulated curve asymptotes to approximately this value, confirming the theoretical expectation. The effective time constant after the pump failure is:

$$\tau_{\text{fail}} = \frac{m}{\epsilon \dot{m}} \approx \frac{20}{0.986 \times 0.01} \approx 2030 \text{ s}$$

so the post-failure rise is slower in normalized time but leads to a much higher final temperature.

Physically, this scenario illustrates that:

- **Radiator effectiveness (ε) increases** as flow decreases (NTU becomes large), but
- **Overall heat removal capacity** $\epsilon \dot{m} C_p$ **collapses** because $\dot{m}$ shrinks dramatically.

Therefore, despite a "high NTU, high ε" radiator, inadequate mass flow inevitably causes dangerous overheating.

3.3. Scenario B (Efficiency Improvement) Results

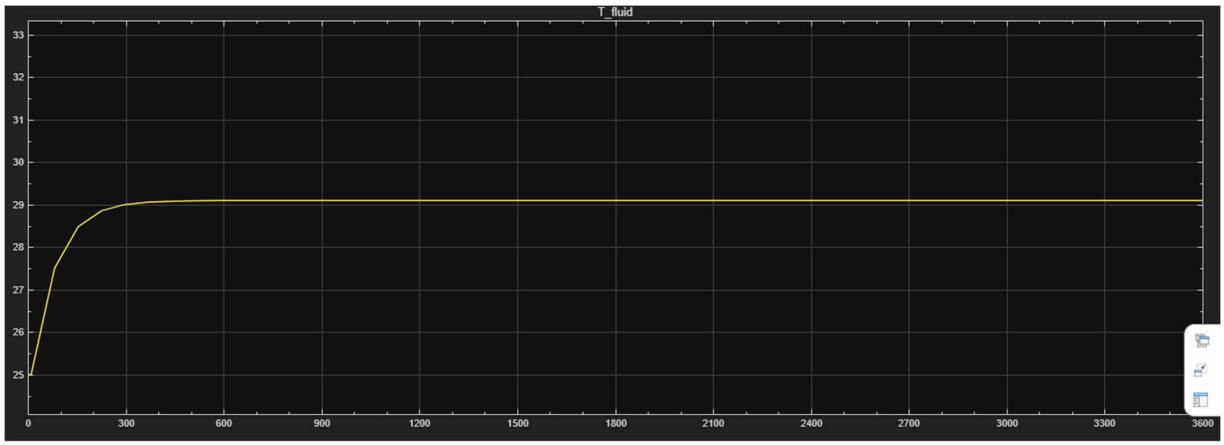

Figure 5: T_{fluid} vs t of the Scenario B Model

In Scenario B, the mass flow remains at 0.2 kg/s, but radiator conductance is doubled to $UA_{\text{rated}} = 300$ W/K. The above figure shows the resulting temperature response. Analytically:

- $C_{\text{rate}} = 700$ W/K(unchanged).
- NTU $= 300/700 \approx 0.429$
- $\epsilon = 1 - e^{-0.429} \approx 0.349$
- $\epsilon C_{\text{rate}} \approx 0.349 \times 700 \approx 244$ W/K
- Steady-state:

$$1000 = 244(T_\infty - 25) \Rightarrow T_\infty - 25 \approx 4.1^\circ\text{C} \Rightarrow T_\infty \approx 29.1^\circ\text{C}$$

The simulated steady temperature is ~29°C, aligning with this prediction. Compared to the base case (32.4°C), doubling UA reduces the coolant temperature by roughly **3.3°C** under the same 1 kW load.

The time constant also decreases:

$$\tau_{\text{improved}} = \frac{m}{\epsilon \dot{m}} \approx \frac{20}{0.349 \times 0.2} \approx 287 \text{ s}$$

so the system settles more quickly, with both a lower peak and lower steady-state temperature.

4.0. Discussion

This subsection discusses the comparative analysis between the base model and two scenarios, as well as the limitations of the project.

4.1. Comparative Analysis of Base Model and Scenarios

Base Model: Based on the results above, the base model achieves a modest temperature rise (~7.4°C above ambient) at 1 kW. It also provides a reasonable margin below typical 40–60°C component limits but may be marginal for high-reliability or high-density applications.

Scenario A (Pump Failure): This demonstrates how a single point of failure in the pump or flow path can lead to an uncontrolled temperature rise above 50°C within tens of minutes. Even though the radiator's theoretical effectiveness improves (NTU increases), the actual heat removal capacity is constrained by the reduced mass flow, causing severe overheating, as seen in the post-failure steady temperature climbs from 32°C to 54°C. This reflects real battery thermal management, where pump failures or coolant loss are highlighted as critical hazards that can accelerate degradation or trigger thermal runaway (Kadhim, 2018; Thermtest, 2024; Williams, 2012).

Scenario B (Efficiency Improvement): This shows that upgrading the heat exchanger (doubling UA) reduces steady-state temperature by ~3.3°C and shortens the time constant, improving both safety margin and transient behavior (Lienhard & Lienhard, 2024; Williams, 2012). This mirrors industrial and data-center practice where higher-performance liquid-to-air or liquid-to-liquid heat exchangers are deployed to support higher rack powers and reuse waste heat (Kadhim, 2018; Gramont, 2026).

An important insight is that **pump reliability and redundancy (Scenario A) matter more for safety** than heat-exchanger upgrades (Scenario B). A system with an excellent radiator but a fragile pumping subsystem can still fail catastrophically, while a robust pumping architecture with a moderate radiator can often maintain acceptable temperatures through redundancy and control.

4.2. Project Limitations

The project model has the following limitations:

- **Well-mixed coolant**: No spatial gradients or channel-to-channel maldistribution are captured; real manifolds can exhibit 20–30% flow imbalance across branches (Azzopardi, 2011).
- **Constant properties:** C_p, density, and UA are taken as temperature-independent; in reality, fluid properties and air-side convection vary with temperature and flow (Direns Mines Paris, 2024).
- **Single lumped heat source:** Multiple components with different thermal masses and limits are aggregated (Arumugam et al., 2023).

5.0. Conclusion

This project developed a dynamic MATLAB/Simulink model of an active liquid cooling loop using lumped-capacitance and effectiveness–NTU theory. The model accurately reproduces first-order thermal behavior and yields closed-form expressions for steady-state temperature and time constant, which match simulation results.

Key insights are:

- Under nominal conditions, a 1 kW load, 20 kg coolant mass, and $UA_{\text{rated}} = 150$ W/K produce a ~7.4°C rise above ambient, settling near 32.4°C.
- A severe pump failure reducing flow from 0.2 to 0.01 kg/s drives coolant temperature toward ~54°C, despite increased radiator effectiveness, demonstrating that pump integrity is critical for safety.
- Doubling radiator conductance to 300 W/K lowers the steady-state temperature to ~29.1°C and shortens the time constant, providing a modest but meaningful improvement in thermal margin and response speed.

The scenarios and their associated plots provide a clear, physically interpretable illustration of how thermal mass, flow rate, and exchanger sizing interact in real cooling systems. The same modeling approach can be extended to more complex multi-node systems and used as a foundation for advanced control and optimization of liquid-cooled data centers, EV battery packs, and industrial power electronics.

REFERENCES

Arumugam, A., Buonomo, B., Luiso, M., & Manca, O. (2023). Lumped capacitance thermal modelling approaches for different cylindrical batteries. *International Journal of Energy Production and Management, 8*(4), 201–210. https://doi.org/10.18280/ijepm.080401

Azzopardi, B.J. (2011). Headers and manifolds, flow distribution in. In *Thermopedia*. Thermopedia Ltd. https://www.thermopedia.com/content/830/

Chandra Sekhar P, A Ramakrishna, 2013, Experimental Investigation Of Liquid Cooling System For Electronics Cooling, International Journal Of Engineering Research & Technology (IJERT) Volume 02, Issue 02 (February 2013)

CoreChem, Inc. (2026). *Ethylene glycol / water mixture properties*. CoreChem. https://corecheminc.com/ethylene-glycol-water-mixture-properties/

Direns Mines Paris. (2024). *Single phase heat exchangers*. Mines Paris – PSL. https://direns.minesparis.psl.eu/Sites/Thopt/en/co/fil-echangeurs.html

EAI Water. (2026). *How to optimize glycol water mixture for maximum efficiency*. EAI Water. https://eaiwater.com/glycol-mixture/

Gramont, A. (2026). *Liquid cooling steps up for high-density racks and AI workloads*. CoreSite. https://www.coresite.com/blog/liquid-cooling-steps-up-for-high-density-racks-and-ai-workloads

Kadhim, M. A. (2018). *Holistic study of thermal management in direct liquid cooled data centres: From the chip to the environment* (Doctoral dissertation, University of Leeds). White Rose eTheses Online. https://etheses.whiterose.ac.uk/id/eprint/21185/

Lienhard, J. H., & Lienhard, J. H. V. (2024). *A heat transfer textbook* (6th ed.). Dover Publications. https://ahtt.mit.edu/

Melinder, Å. (2007). *Thermophysical properties of aqueous solutions used as heat transfer fluids* (Doctoral dissertation, Royal Institute of Technology). KTH. https://www.diva-portal.org/smash/get/diva2:12169/fulltext01.pdf

Neural Concept. (2026). *What is battery cooling and how does it work?* Neural Concept. https://www.neuralconcept.com/post/what-is-battery-liquid-cooling-and-how-does-it-work

P. A. Hilton (2026). *Water to air heat exchanger*. https://www.p-a-hilton.co.uk/products/heat-transfer/water-air-heat-exchanger

SinoExtrud. (2025). *What is the optimal flow rate for liquid cooling plates?* SinoExtrud. https://sinoextrud.com/what-is-the-optimal-flow-rate-for-liquid-cooling-plates/

The Engineering ToolBox (2003). *Ethylene Glycol Heat-Transfer Fluid Properties: Density, Data & Charts*. [online] Available at: https://www.engineeringtoolbox.com/ethylene-glycol-d_146.html [Accessed 3rd January, 2026]

Thermtest. (2024, December 8). *Battery thermal management: Everything you need to know*. Thermtest Inc. https://thermtest.com/battery-thermal-management-system

Williams, B. W. (2012). *High performance cooling for power electronics* (Chapter 6). In *Power electronics: Devices, drivers, applications, and passive components* (Course notes). University of Strathclyde. https://personal.eee.strath.ac.uk/barry.williams/Book/Chapter%206.pdf